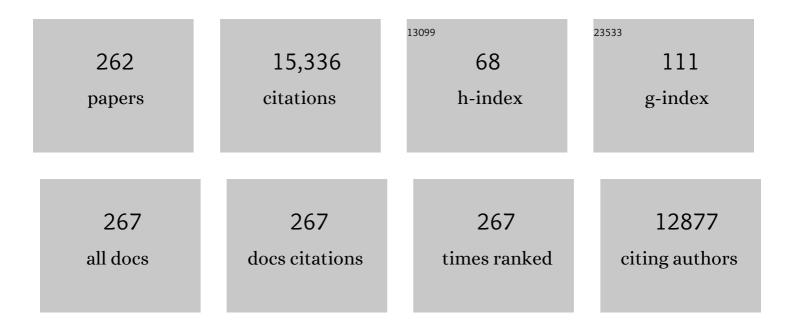
List of Publications by Year in descending order

Source: https://exaly.com/author-pdf/3918405/publications.pdf Version: 2024-02-01



RENIAMIN HSIAO

#	Article	IF	CITATIONS
1	NANOFIBROUS MATERIALS AND THEIR APPLICATIONS. Annual Review of Materials Research, 2006, 36, 333-368.	9.3	573
2	High flux ultrafiltration membranes based on electrospun nanofibrous PAN scaffolds and chitosan coating. Polymer, 2006, 47, 2434-2441.	3.8	503
3	Functional nanofibers for environmental applications. Journal of Materials Chemistry, 2008, 18, 5326.	6.7	388
4	Small-Angle X-ray Scattering of Polymers. Chemical Reviews, 2001, 101, 1727-1762.	47.7	348
5	Isothermal Crystallization of Poly(<scp>l</scp> -lactide) Induced by Graphene Nanosheets and Carbon Nanotubes: A Comparative Study. Macromolecules, 2010, 43, 5000-5008.	4.8	308
6	Unexpected Shish-Kebab Structure in a Sheared Polyethylene Melt. Physical Review Letters, 2005, 94, 117802.	7.8	254
7	Effects of organoclays on morphology and thermal and rheological properties of polystyrene and poly(methyl methacrylate) blends. Journal of Polymer Science, Part B: Polymer Physics, 2003, 41, 44-54.	2.1	250
8	Ultra-fine cellulose nanofibers: new nano-scale materials for water purification. Journal of Materials Chemistry, 2011, 21, 7507.	6.7	250
9	Micro-nano structure poly(ether sulfones)/poly(ethyleneimine) nanofibrous affinity membranes for adsorption of anionic dyes and heavy metal ions in aqueous solution. Chemical Engineering Journal, 2012, 197, 88-100.	12.7	250
10	Nanofibrous microfiltration membranes capable of removing bacteria, viruses and heavy metal ions. Journal of Membrane Science, 2013, 446, 376-382.	8.2	215
11	Ultrafine Polysaccharide Nanofibrous Membranes for Water Purification. Biomacromolecules, 2011, 12, 970-976.	5.4	212
12	Thiol-modified cellulose nanofibrous composite membranes for chromium (VI) and lead (II) adsorption. Polymer, 2014, 55, 1167-1176.	3.8	211
13	Nanofibrous Microfiltration Membrane Based on Cellulose Nanowhiskers. Biomacromolecules, 2012, 13, 180-186.	5.4	201
14	Ultrafine Cellulose Nanofibers as Efficient Adsorbents for Removal of UO ₂ ²⁺ in Water. ACS Macro Letters, 2012, 1, 213-216.	4.8	187
15	Nanoscale reinforcement of polyhedral oligomeric silsesquioxane (POSS) in polyurethane elastomer. Polymer International, 2000, 49, 437-440.	3.1	182
16	Formation and Stability of Shear-Induced Shish-Kebab Structure in Highly Entangled Melts of UHMWPE/HDPE Blends. Macromolecules, 2008, 41, 4766-4776.	4.8	162
17	Graphene Nanosheets and Shear Flow Induced Crystallization in Isotactic Polypropylene Nanocomposites. Macromolecules, 2011, 44, 2808-2818.	4.8	160
18	Formation of functional polyethersulfone electrospun membrane for water purification by mixed solvent and oxidation processes. Polymer, 2009, 50, 2893-2899.	3.8	156

#	Article	IF	CITATIONS
19	Highly Permeable Polymer Membranes Containing Directed Channels for Water Purification. ACS Macro Letters, 2012, 1, 723-726.	4.8	154
20	Effective chromium removal from water by polyaniline-coated electrospun adsorbent membrane. Chemical Engineering Journal, 2019, 372, 341-351.	12.7	151
21	Fabrication and characterization of cellulose nanofiber based thin-film nanofibrous composite membranes. Journal of Membrane Science, 2014, 454, 272-282.	8.2	150
22	Unprecedented Access to Strong and Ductile Poly(lactic acid) by Introducing In Situ Nanofibrillar Poly(butylene succinate) for Green Packaging. Biomacromolecules, 2014, 15, 4054-4064.	5.4	149
23	Functionalized electrospun nanofibrous microfiltration membranes for removal of bacteria and viruses. Journal of Membrane Science, 2014, 452, 446-452.	8.2	142
24	Dual-Biomimetic Superhydrophobic Electrospun Polystyrene Nanofibrous Membranes for Membrane Distillation. ACS Applied Materials & Interfaces, 2014, 6, 2423-2430.	8.0	141
25	Mechanism of strain-induced crystallization in filled and unfilled natural rubber vulcanizates. Journal of Applied Physics, 2005, 97, 103529.	2.5	140
26	Low-dimensional carbonaceous nanofiller induced polymer crystallization. Progress in Polymer Science, 2014, 39, 555-593.	24.7	140
27	Nanocellulose from Spinifex as an Effective Adsorbent to Remove Cadmium(II) from Water. ACS Sustainable Chemistry and Engineering, 2018, 6, 3279-3290.	6.7	138
28	Crystallization studies of isotactic polypropylene containing nanostructured polyhedral oligomeric silsesquioxane molecules under quiescent and shear conditions. Journal of Polymer Science, Part B: Polymer Physics, 2001, 39, 2727-2739.	2.1	135
29	Electrospinning of Hyaluronic Acid (HA) and HA/Gelatin Blends. Macromolecular Rapid Communications, 2006, 27, 114-120.	3.9	134
30	Entanglements and Networks to Strain-Induced Crystallization and Stress–Strain Relations in Natural Rubber and Synthetic Polyisoprene at Various Temperatures. Macromolecules, 2013, 46, 5238-5248.	4.8	132
31	Mesophase as the Precursor for Strain-Induced Crystallization in Amorphous Poly(ethylene) Tj ETQq1 1 0.78431	4 rgBT /Ov	verlock 10 Tf 5
32	Competitive Growth of α- and β-Crystals in β-Nucleated Isotactic Polypropylene under Shear Flow. Macromolecules, 2010, 43, 6760-6771.	4.8	128
33	Formation of Shish-Kebabs in Injection-Molded Poly(<scp>l</scp> -lactic acid) by Application of an Intense Flow Field. ACS Applied Materials & amp; Interfaces, 2012, 4, 6774-6784.	8.0	128
34	High-flux thin-film nanofibrous composite ultrafiltration membranes containing cellulose barrier layer. Journal of Materials Chemistry, 2010, 20, 4692.	6.7	125
35	A Simple Approach to Prepare Carboxycellulose Nanofibers from Untreated Biomass. Biomacromolecules, 2017, 18, 2333-2342.	5.4	124
36	Nanocelluloseâ€Enabled Membranes for Water Purification: Perspectives. Advanced Sustainable Systems, 2020, 4, 1900114.	5.3	118

#	Article	IF	CITATIONS
37	Characterization of Nanocellulose Using Small-Angle Neutron, X-ray, and Dynamic Light Scattering Techniques. Journal of Physical Chemistry B, 2017, 121, 1340-1351.	2.6	112
38	High performance thin-film nanofibrous composite hemodialysis membranes with efficient middle-molecule uremic toxin removal. Journal of Membrane Science, 2017, 523, 173-184.	8.2	111
39	Nanofibrous polydopamine complex membranes for adsorption of Lanthanum (III) ions. Chemical Engineering Journal, 2014, 244, 307-316.	12.7	106
40	Nature of Strain-Induced Structures in Natural and Synthetic Rubbers under Stretching. Macromolecules, 2003, 36, 5915-5917.	4.8	104
41	In vitro non-viral gene delivery with nanofibrous scaffolds. Nucleic Acids Research, 2005, 33, e170-e170.	14.5	102
42	Thermal Stability of Shear-Induced Shish-Kebab Precursor Structure from High Molecular Weight Polyethylene Chains. Macromolecules, 2006, 39, 2209-2218.	4.8	102
43	Super-Robust Polylactide Barrier Films by Building Densely Oriented Lamellae Incorporated with Ductile in Situ Nanofibrils of Poly(butylene adipate- <i>co</i> -terephthalate). ACS Applied Materials & Interfaces, 2016, 8, 8096-8109.	8.0	102
44	Fabrication of thin-film nanofibrous composite membranes by interfacial polymerization using ionic liquids as additives. Journal of Membrane Science, 2010, 365, 52-58.	8.2	98
45	Structure Development during the Melt Spinning of Polyethylene and Poly(vinylidene fluoride) Fibers by in Situ Synchrotron Small- and Wide-Angle X-ray Scattering Techniques. Macromolecules, 1999, 32, 8121-8132.	4.8	96
46	Efficient Removal of Arsenic Using Zinc Oxide Nanocrystal-Decorated Regenerated Microfibrillated Cellulose Scaffolds. ACS Sustainable Chemistry and Engineering, 2019, 7, 6140-6151.	6.7	93
47	Understanding the Mechanistic Behavior of Highly Charged Cellulose Nanofibers in Aqueous Systems. Macromolecules, 2018, 51, 1498-1506.	4.8	92
48	Novel nanofibrous scaffolds for water filtration with bacteria and virus removal capability. Journal of Electron Microscopy, 2011, 60, 201-209.	0.9	90
49	Effect of Network-Chain Length on Strain-Induced Crystallization of NR and IR Vulcanizates. Rubber Chemistry and Technology, 2004, 77, 711-723.	1.2	89
50	In Situ Synchrotron X-ray Scattering Study on Isotactic Polypropylene Crystallization under the Coexistence of Shear Flow and Carbon Nanotubes. Macromolecules, 2011, 44, 8080-8092.	4.8	89
51	Strong Shear Flow-Driven Simultaneous Formation of Classic Shish-Kebab, Hybrid Shish-Kebab, and Transcrystallinity in Poly(lactic acid)/Natural Fiber Biocomposites. ACS Sustainable Chemistry and Engineering, 2013, 1, 1619-1629.	6.7	89
52	Strain-Induced Crystallization of Natural Rubber: Effect of Proteins and Phospholipids. Rubber Chemistry and Technology, 2008, 81, 753-766.	1.2	88
53	Highly efficient and sustainable carboxylated cellulose filters for removal of cationic dyes/heavy metals ions. Chemical Engineering Journal, 2020, 389, 123458.	12.7	88
54	Enhanced Mechanical Performance of Selfâ€Bundled Electrospun Fiber Yarns via Postâ€Treatments. Macromolecular Rapid Communications, 2008, 29, 826-831.	3.9	87

#	Article	IF	CITATIONS
55	Design and fabrication of electrospun polyethersulfone nanofibrous scaffold for highâ€flux nanofiltration membranes. Journal of Polymer Science, Part B: Polymer Physics, 2009, 47, 2288-2300.	2.1	84
56	Thin-film nanofibrous composite membranes containing cellulose or chitin barrier layers fabricated by ionic liquids. Polymer, 2011, 52, 2594-2599.	3.8	84
57	High flux ethanol dehydration using nanofibrous membranes containing graphene oxide barrier layers. Journal of Materials Chemistry A, 2013, 1, 12998.	10.3	84
58	Self-roughened omniphobic coatings on nanofibrous membrane for membrane distillation. Separation and Purification Technology, 2018, 206, 14-25.	7.9	82
59	Nanocellulose for Sustainable Water Purification. Chemical Reviews, 2022, 122, 8936-9031.	47.7	82
60	Study of the structure development during the melt spinning of nylon 6 fiber by on-line wide-angle synchrotron X-ray scattering techniques. Journal of Polymer Science, Part B: Polymer Physics, 1999, 37, 1277-1287.	2.1	80
61	Nanofibrous ultrafiltration membranes containing cross-linked poly(ethylene glycol) and cellulose nanofiber composite barrier layer. Polymer, 2014, 55, 366-372.	3.8	80
62	Nanofiltration membranes based on thin-film nanofibrous composites. Journal of Membrane Science, 2014, 469, 188-197.	8.2	80
63	Efficient Removal of UO ₂ ²⁺ from Water Using Carboxycellulose Nanofibers Prepared by the Nitro-Oxidation Method. Industrial & Engineering Chemistry Research, 2017, 56, 13885-13893.	3.7	79
64	Single Molecular Layer of Silk Nanoribbon as Potential Basic Building Block of Silk Materials. ACS Nano, 2018, 12, 11860-11870.	14.6	79
65	Interfacial Shish-Kebabs Lengthened by Coupling Effect of In Situ Flexible Nanofibrils and Intense Shear Flow: Achieving Hierarchy To Conquer the Conflicts between Strength and Toughness of Polylactide. ACS Applied Materials & Interfaces, 2017, 9, 10148-10159.	8.0	77
66	Eco-friendly poly(acrylic acid)-sodium alginate nanofibrous hydrogel: A multifunctional platform for superior removal of Cu(II) and sustainable catalytic applications. Colloids and Surfaces A: Physicochemical and Engineering Aspects, 2018, 558, 228-241.	4.7	74
67	Anionic Surfactant-Triggered Steiner Geometrical Poly(vinylidene fluoride) Nanofiber/Nanonet Air Filter for Efficient Particulate Matter Removal. ACS Applied Materials & Interfaces, 2018, 10, 42891-42904.	8.0	73
68	Highly permeable nanofibrous composite microfiltration membranes for removal of nanoparticles and heavy metal ions. Separation and Purification Technology, 2020, 233, 115976.	7.9	72
69	Silver Nanoparticle-Enabled Photothermal Nanofibrous Membrane for Light-Driven Membrane Distillation. Industrial & Engineering Chemistry Research, 2019, 58, 3269-3281.	3.7	70
70	Thiol-functionalized chitin nanofibers for As (III) adsorption. Polymer, 2015, 60, 9-17.	3.8	69
71	Superior Impact Toughness and Excellent Storage Modulus of Poly(lactic acid) Foams Reinforced by Shish-Kebab Nanoporous Structure. ACS Applied Materials & Interfaces, 2017, 9, 21071-21076.	8.0	69
72	Thin-film nanofibrous composite reverse osmosis membranes for desalination. Desalination, 2017, 420, 91-98.	8.2	69

#	Article	IF	CITATIONS
73	Lead removal from water using carboxycellulose nanofibers prepared by nitro-oxidation method. Cellulose, 2018, 25, 1961-1973.	4.9	69
74	From Nanofibrillar to Nanolaminar Poly(butylene succinate): Paving the Way to Robust Barrier and Mechanical Properties for Full-Biodegradable Poly(lactic acid) Films. ACS Applied Materials & Interfaces, 2015, 7, 8023-8032.	8.0	67
75	Integrated polyamide thin-film nanofibrous composite membrane regulated by functionalized interlayer for efficient water/isopropanol separation. Journal of Membrane Science, 2018, 553, 70-81.	8.2	67
76	Structure Changes during Uniaxial Deformation of Ethylene-Based Semicrystalline Ethyleneâ^'Propylene Copolymer. 1. SAXS Study. Macromolecules, 2003, 36, 1920-1929.	4.8	66
77	Arsenic(III) Removal by Nanostructured Dialdehyde Cellulose–Cysteine Microscale and Nanoscale Fibers. ACS Omega, 2019, 4, 22008-22020.	3.5	66
78	Dislocation-Controlled Perforated Layer Phase in a PEO- b-PS Diblock Copolymer. Physical Review Letters, 2001, 86, 6030-6033.	7.8	63
79	Low pressure UV-cured CS–PEO–PTEGDMA/PAN thin film nanofibrous composite nanofiltration membranes for anionic dye separation. Journal of Materials Chemistry A, 2016, 4, 15575-15588.	10.3	62
80	Structural developments in synthetic rubbers during uniaxial deformation byin situ synchrotron X-ray diffraction. Journal of Polymer Science, Part B: Polymer Physics, 2004, 42, 956-964.	2.1	61
81	Real-Time Crystallization of Organoclay Nanoparticle Filled Natural Rubber under Stretching. Macromolecules, 2008, 41, 2295-2298.	4.8	61
82	Electrospun Nanofibrous Membrane for Heavy Metal Ion Adsorption. Current Organic Chemistry, 2013, 17, 1361-1370.	1.6	61
83	Strong and tough micro/nanostructured poly(lactic acid) by mimicking the multifunctional hierarchy of shell. Materials Horizons, 2014, 1, 546-552.	12.2	61
84	Molecular dynamics and microstructure development during cold crystallization in poly(ether-ether-ketone) as revealed by real time dielectric and x-ray methods. Journal of Chemical Physics, 2001, 115, 3804-3813.	3.0	59
85	Multiâ€scaled microstructures in natural rubber characterized by synchrotron Xâ€ray scattering and optical microscopy. Journal of Polymer Science, Part B: Polymer Physics, 2008, 46, 2456-2464.	2.1	59
86	Crystal and Crystallites Structure of Natural Rubber and Synthetic <i>cis</i> -1,4-Polyisoprene by a New Two Dimensional Wide Angle X-ray Diffraction Simulation Method. I. Strain-Induced Crystallization. Macromolecules, 2013, 46, 4520-4528.	4.8	59
87	Structure characterization of cellulose nanofiber hydrogel as functions of concentration and ionic strength. Cellulose, 2017, 24, 5417-5429.	4.9	59
88	New Insights into Lamellar Structure Development and SAXS/WAXD Sequence Appearance during Uniaxial Stretching of Amorphous Poly(ethylene terephthalate) above Glass Transition Temperature. Macromolecules, 2008, 41, 2859-2867.	4.8	58
89	Cationic Dialdehyde Nanocellulose from Sugarcane Bagasse for Efficient Chromium(VI) Removal. ACS Sustainable Chemistry and Engineering, 2020, 8, 4734-4744.	6.7	58
90	Role of Stably Entangled Chain Network Density in Shish-Kebab Formation in Polyethylene under an Intense Flow Field. Macromolecules, 2015, 48, 6652-6661.	4.8	57

#	Article	IF	CITATIONS
91	Effects of Block Architecture on Structure and Mechanical Properties of Olefin Block Copolymers under Uniaxial Deformation. Macromolecules, 2011, 44, 3670-3673.	4.8	55
92	Ultra-fine electrospun nanofibrous membranes for multicomponent wastewater treatment: Filtration and Aurification Technology, 2020, 242, 116794.	7.9	53
93	Super-hydrophobic modification of porous natural polymer "luffa sponge―for oil absorption. Polymer, 2017, 126, 470-476.	3.8	52
94	Robust superhydrophobic dual layer nanofibrous composite membranes with a hierarchically structured amorphous polypropylene skin for membrane distillation. Journal of Materials Chemistry A, 2019, 7, 11282-11297.	10.3	52
95	Structure development during melt spinning and subsequent annealing of polybutene-1 fibers. Journal of Polymer Science, Part B: Polymer Physics, 2000, 38, 1872-1882.	2.1	49
96	Characterization of TEMPO-oxidized cellulose nanofibers in aqueous suspension by small-angle X-ray scattering. Journal of Applied Crystallography, 2014, 47, 788-798.	4.5	49
97	Exploring the Nature of Cellulose Microfibrils. Biomacromolecules, 2015, 16, 1201-1209.	5.4	48
98	Nature of Shear-Induced Primary Nuclei in iPP Melt. Journal of Macromolecular Science - Physics, 2003, 42, 515-531.	1.0	47
99	Thin-Film Nanofibrous Composite Ultrafiltration Membranes Based on Polyvinyl Alcohol Barrier Layer Containing Directional Water Channels. Industrial & Engineering Chemistry Research, 2010, 49, 11978-11984.	3.7	47
100	Molecular dynamics of natural rubber as revealed by dielectric spectroscopy: The role of natural cross–linking. Soft Matter, 2010, 6, 3636.	2.7	47
101	High Aspect Ratio Carboxycellulose Nanofibers Prepared by Nitro-Oxidation Method and Their Nanopaper Properties. ACS Applied Nano Materials, 2018, 1, 3969-3980.	5.0	47
102	Molecular orientation and stress relaxation during strain-induced crystallization of vulcanized natural rubber. Polymer Journal, 2010, 42, 474-481.	2.7	46
103	Real-Time Structure Changes during Uniaxial Stretching of Poly(ω-pentadecalactone) by <i>in Situ</i> Synchrotron WAXD/SAXS Techniques. Macromolecules, 2011, 44, 3874-3883.	4.8	46
104	Antifouling nanocellulose membranes: How subtle adjustment of surface charge lead to self-cleaning property. Journal of Membrane Science, 2021, 618, 118739.	8.2	46
105	The role of polymers in breakthrough technologies for water purification. Journal of Polymer Science, Part B: Polymer Physics, 2009, 47, 2431-2435.	2.1	45
106	Crystal and Crystallites Structure of Natural Rubber and Peroxide-Vulcanized Natural Rubber by a Two-Dimensional Wide-Angle X-ray Diffraction Simulation Method. II. Strain-Induced Crystallization versus Temperature-Induced Crystallization. Macromolecules, 2013, 46, 9712-9721.	4.8	45
107	Cross-Sections of Nanocellulose from Wood Analyzed by Quantized Polydispersity of Elementary Microfibrils. ACS Nano, 2020, 14, 16743-16754.	14.6	45
108	Continuous fabrication of cellulose nanocrystal/poly(ethylene glycol) diacrylate hydrogel fiber from nanocomposite dispersion: Rheology, preparation and characterization. Polymer, 2017, 123, 55-64.	3.8	44

#	Article	IF	CITATIONS
109	In Vitro Mineralization of Collagen in Demineralized Fish Bone. Macromolecular Chemistry and Physics, 2005, 206, 43-51.	2.2	43
110	Shear-Induced Precursor Relaxation-Dependent Growth Dynamics and Lamellar Orientation of β-Crystals in β-Nucleated Isotactic Polypropylene. Journal of Physical Chemistry B, 2015, 119, 5716-5727.	2.6	43
111	In Situ Nanofibrillar Networks Composed of Densely Oriented Polylactide Crystals as Efficient Reinforcement and Promising Barrier Wall for Fully Biodegradable Poly(butylene succinate) Composite Films. ACS Sustainable Chemistry and Engineering, 2016, 4, 2887-2897.	6.7	43
112	Novel thin-film nanofibrous composite membranes containing directional toxin transport nanochannels for efficient and safe hemodialysis application. Journal of Membrane Science, 2019, 582, 151-163.	8.2	43
113	Elucidating the Opportunities and Challenges for Nanocellulose Spinning. Advanced Materials, 2021, 33, e2001238.	21.0	43
114	Facile synthesis of TiO2/CNC nanocomposites for enhanced Cr(VI) photoreduction: Synergistic roles of cellulose nanocrystals. Carbohydrate Polymers, 2020, 233, 115838.	10.2	43
115	Preferred Orientation in Polymer Fiber Scattering. Polymer Reviews, 2010, 50, 91-111.	10.9	42
116	Strong Silk Fibers Containing Cellulose Nanofibers Generated by a Bioinspired Microfluidic Chip. ACS Sustainable Chemistry and Engineering, 2019, 7, 14765-14774.	6.7	42
117	Tough and Elastic Thermoplastic Organogels and Elastomers Made of Semicrystalline Polyolefin-Based Block Copolymers. Macromolecules, 2012, 45, 5604-5618.	4.8	41
118	Molecular Weight and Crystallization Temperature Effects on Poly(ethylene terephthalate) (PET) Homopolymers, an Isothermal Crystallization Analysis. Polymers, 2014, 6, 583-600.	4.5	41
119	Engineering construction of robust superhydrophobic two-tier composite membrane with interlocked structure for membrane distillation. Journal of Membrane Science, 2020, 598, 117813.	8.2	41
120	Biodegradable silk fibroin-based bio-piezoelectric/triboelectric nanogenerators as self-powered electronic devices. Nano Energy, 2022, 96, 107101.	16.0	41
121	In-Situ X-ray Deformation Study of Fluorinated Multiwalled Carbon Nanotube and Fluorinated Ethyleneâ^ Propylene Nanocomposite Fibers. Macromolecules, 2006, 39, 5427-5437.	4.8	40
122	Biofouling-resistant nanocellulose layer in hierarchical polymeric membranes: Synthesis, characterization and performance. Journal of Membrane Science, 2019, 579, 162-171.	8.2	40
123	A durable thin-film nanofibrous composite nanofiltration membrane prepared by interfacial polymerization on a double-layer nanofibrous scaffold. RSC Advances, 2017, 7, 18001-18013.	3.6	39
124	Processingâ€structureâ€mechanical property relationships of semicrystalline polyolefinâ€based block copolymers. Journal of Polymer Science, Part B: Polymer Physics, 2010, 48, 1428-1437.	2.1	38
125	Plastic Deformation of Semicrystalline Polyethylene by X-ray Scattering: Comparison with Atomistic Simulations. Macromolecules, 2013, 46, 5279-5289.	4.8	38
126	Simultaneous improvement of strength and toughness in fiber reinforced isotactic polypropylene composites by shear flow and a \hat{l}^2 -nucleating agent. RSC Advances, 2014, 4, 14766-14776.	3.6	38

#	Article	IF	CITATIONS
127	Step-Cycle Mechanical Processing of Gels of sPP- <i>b</i> -EPR- <i>b</i> -sPP Triblock Copolymer in Mineral Oil. Macromolecules, 2010, 43, 6782-6788.	4.8	37
128	Chain Dynamics and Strain-Induced Crystallization of Pre- and Postvulcanized Natural Rubber Latex Using Proton Multiple Quantum NMR and Uniaxial Deformation by <i>in Situ</i> Synchrotron X-ray Diffraction. Macromolecules, 2012, 45, 6491-6503.	4.8	36
129	Improvement of meltdown temperature of lithium-ion battery separator using electrospun polyethersulfone membranes. Polymer, 2016, 107, 163-169.	3.8	36
130	Integrated dynamic wet spinning of core-sheath hydrogel fibers for optical-to-brain/tissue communications. National Science Review, 2021, 8, nwaa209.	9.5	36
131	Insight into unique deformation behavior of oriented isotactic polypropylene with branched shish-kebabs. Polymer, 2015, 60, 274-283.	3.8	35
132	DETERMINATION OF CRYSTALLINE LAMELLAR THICKNESS IN POLY(ETHYLENE TEREPHTHALATE) USING SMALL-ANGLE X-RAY SCATTERING AND TRANSMISSION ELECTRON MICROSCOPY*. Journal of Macromolecular Science - Physics, 2001, 40, 625-638.	1.0	33
133	Crystallization of Polystyrene-block-[Syndiotactic Poly(propylene)] Block Copolymers from Confinement to Breakout. Macromolecular Rapid Communications, 2005, 26, 107-111.	3.9	33
134	Large Scale Production of Continuous Hydrogel Fibers with Anisotropic Swelling Behavior by Dynamic rosslinking‧pinning. Macromolecular Rapid Communications, 2016, 37, 1795-1801.	3.9	33
135	Enhanced pervaporation performance of polyamide membrane with synergistic effect of porous nanofibrous support and trace graphene oxide lamellae. Chemical Engineering Science, 2019, 196, 265-276.	3.8	33
136	Competition between liquid crystallinity and block copolymerself-assembly in core–shell rod–coil block copolymers. Soft Matter, 2008, 4, 458-461.	2.7	32
137	Phase Behavior of Neat Triblock Copolymers and Copolymer/Homopolymer Blends Near Network Phase Windows. Macromolecules, 2010, 43, 9039-9048.	4.8	32
138	Time-Resolved Synchrotron X-ray Scattering Study on Propylene–1-Butylene Random Copolymer Subjected to Uniaxial Stretching at High Temperatures. Macromolecules, 2012, 45, 951-961.	4.8	32
139	Morphology development during isothermal crystallization. I. Isotactic and atactic polypropylene blends. Journal of Polymer Science, Part B: Polymer Physics, 2000, 38, 2580-2590.	2.1	31
140	Title is missing!. Journal of Materials Science, 2001, 36, 3071-3077.	3.7	31
141	Shearâ€Induced Orientation and Structure Development in Isotactic Polypropylene Melt Containing Modified Carbon Nanofibers. Journal of Macromolecular Science - Physics, 2006, 45, 247-261.	1.0	31
142	Polypentadecalactone prepared by lipase catalysis: crystallization kinetics and morphology. Polymer International, 2009, 58, 944-953.	3.1	31
143	Biodegradable poly(lactic acid)/hydroxyl apatite 3D porous scaffolds using high-pressure molding and salt leaching. Journal of Materials Science, 2014, 49, 1648-1658.	3.7	31
144	Structure and morphology development in syndiotactic polypropylene during isothermal crystallization and subsequent melting. Journal of Polymer Science, Part B: Polymer Physics, 2001, 39, 2982-2995.	2.1	30

#	Article	IF	CITATIONS
145	Pathway-Dependent Melting in a Low-Molecular-Weight Polyethylene-block-Poly(ethylene oxide) Diblock Copolymer. Macromolecular Rapid Communications, 2004, 25, 853-857.	3.9	30
146	Nano-Structural Elucidation in Carbon Black Loaded NR Vulcanizate by 3D-TEM and In Situ WAXD Measurements. Rubber Chemistry and Technology, 2007, 80, 251-264.	1.2	30
147	Micro-nano structure nanofibrous p-sulfonatocalix[8]arene complex membranes for highly efficient and selective adsorption of lanthanum(<scp>iii</scp>) ions in aqueous solution. RSC Advances, 2015, 5, 21178-21188.	3.6	30
148	Rice husk based nanocellulose scaffolds for highly efficient removal of heavy metal ions from contaminated water. Environmental Science: Water Research and Technology, 2020, 6, 3080-3090.	2.4	30
149	Effect of miscible polymer diluents on the development of lamellar morphology in poly(oxymethylene) blends. Journal of Polymer Science, Part B: Polymer Physics, 1999, 37, 3115-3122.	2.1	29
150	Probing Flow-Induced Precursor Structures in Blown Polyethylene Films by Synchrotron X-rays during Constrained Melting. Macromolecules, 2005, 38, 5128-5136.	4.8	29
151	Ultra-strong, tough and high wear resistance high-density polyethylene for structural engineering application: A facile strategy towards using the combination of extensional dynamic oscillatory shear flow and ultra-high-molecular-weight polyethylene. Composites Science and Technology, 2018, 167, 301-312.	7.8	29
152	A study of TiO ₂ nanocrystal growth and environmental remediation capability of TiO ₂ /CNC nanocomposites. RSC Advances, 2019, 9, 40565-40576.	3.6	29
153	A simple inorganic hybrids strategy for graphene fibers fabrication with excellent electrochemical performance. Journal of Power Sources, 2020, 450, 227637.	7.8	29
154	Hierarchical Assembly of Nanocellulose into Filaments by Flow-Assisted Alignment and Interfacial Complexation: Conquering the Conflicts between Strength and Toughness. ACS Applied Materials & Interfaces, 2020, 12, 32090-32098.	8.0	29
155	Nanoparticle–Nanofibrous Membranes as Scaffolds for Flexible Sweat Sensors. ACS Sensors, 2016, 1, 1060-1069.	7.8	28
156	Operation of proton exchange membrane (PEM) fuel cells using natural cellulose fiber membranes. Sustainable Energy and Fuels, 2019, 3, 2725-2732.	4.9	28
157	Primary Nucleation in Polymer Crystallization. Macromolecular Rapid Communications, 2001, 22, 611-615.	3.9	26
158	Membrane Bioreactors for Nitrogen Removal from Wastewater: A Review. Journal of Environmental Engineering, ASCE, 2020, 146, .	1.4	26
159	Cellulose nanofibrils and nanocrystals in confined flow: Single-particle dynamics to collective alignment revealed through scanning small-angle x-ray scattering and numerical simulations. Physical Review E, 2020, 101, 032610.	2.1	26
160	Nitro-oxidized carboxycellulose nanofibers from moringa plant: effective bioadsorbent for mercury removal. Cellulose, 2021, 28, 8611-8628.	4.9	26
161	Aligned and molecularly oriented semihollow ultrafine polymer fiber yarns by a facile method. Journal of Polymer Science, Part B: Polymer Physics, 2010, 48, 1118-1125.	2.1	25
162	High-performance nanofibrous membrane for removal of Cr(VI) from contaminated water. Journal of Plastic Film and Sheeting, 2015, 31, 379-400.	2.2	25

#	Article	IF	CITATIONS
163	Synthesis and Characterization of a High Flux Nanocellulose–Cellulose Acetate Nanocomposite Membrane. Membranes, 2019, 9, 70.	3.0	25
164	Molecular Structure of Aromatic Reverse Osmosis Polyamide Barrier Layers. ACS Macro Letters, 2019, 8, 352-356.	4.8	25
165	Heparinized thin-film composite membranes with sub-micron ridge structure for efficient hemodialysis. Journal of Membrane Science, 2020, 599, 117706.	8.2	25
166	Crystallization and phase behavior in nylon 6/aromatic polyimide triblock copolymers. Macromolecular Chemistry and Physics, 1998, 199, 1107-1118.	2.2	24
167	Structure Development during Stretching and Heating of Isotactic Propylene–1-Butylene Random Copolymer: From Unit Cells to Lamellae. Macromolecules, 2012, 45, 7061-7071.	4.8	24
168	Biomimetic Nanofibrillation in Two-Component Biopolymer Blends with Structural Analogs to Spider Silk. Scientific Reports, 2016, 6, 34572.	3.3	24
169	Super-hydrophobic polyurethane sponges for oil absorption. Separation Science and Technology, 2017, 52, 221-227.	2.5	24
170	Interpenetrating Nanofibrous Composite Membranes for Water Purification. ACS Applied Nano Materials, 2019, 2, 3606-3614.	5.0	24
171	Reinforcement of Natural Rubber Latex Using Jute Carboxycellulose Nanofibers Extracted Using Nitro-Oxidation Method. Nanomaterials, 2020, 10, 706.	4.1	24
172	Morphology development during isothermal crystallization. II. Isotactic and syndiotactic polypropylene blends. Journal of Polymer Science, Part B: Polymer Physics, 2001, 39, 1876-1888.	2.1	23
173	Time-resolved crystallization study of absorbable polymers by synchrotron small-angle X-ray scattering. Journal of Polymer Science, Part B: Polymer Physics, 2001, 39, 153-167.	2.1	23
174	Combined techniques of Raman spectroscopy and synchrotron two-dimensional x-ray diffraction forin situstudy of anisotropic system: Example of polymer fibers under deformation. Review of Scientific Instruments, 2003, 74, 3087-3092.	1.3	22
175	Nanocomposite Film Containing Fibrous Cellulose Scaffold and Ag/TiO2 Nanoparticles and Its Antibacterial Activity. Polymers, 2018, 10, 1052.	4.5	22
176	The role of multi-walled carbon nanotubes in shear enhanced crystallization of isotactic poly(1-butene). Journal of Thermal Analysis and Calorimetry, 2009, 98, 611-622.	3.6	21
177	Orientated crystallization in discontinuous aramid fiber/isotactic polypropylene composites under shear flow conditions. Journal of Applied Polymer Science, 2005, 98, 1113-1118.	2.6	20
178	Lamellar nanostructure in 'Somasif'-based organoclays. Clays and Clay Minerals, 2007, 55, 140-150.	1.3	20
179	Morphological and property investigations of carboxylated cellulose nanofibers extracted from different biological species. Cellulose, 2015, 22, 3127-3135.	4.9	20
180	Fabrication of cellulose nanofiberâ€based ultrafiltration membranes by spray coating approach. Journal of Applied Polymer Science, 2017, 134, .	2.6	20

#	Article	IF	CITATIONS
181	In situ synchrotron SAXS/WAXD studies during melt spinning of modified carbon nanofiber and isotactic polypropylene nanocomposite. Colloid and Polymer Science, 2004, 282, 802-809.	2.1	19
182	Morphology and Flow Behavior of Cellulose Nanofibers Dispersed in Glycols. Macromolecules, 2019, 52, 5499-5509.	4.8	18
183	Structural characterization of carboxyl cellulose nanofibers extracted from underutilized sources. Science China Technological Sciences, 2019, 62, 971-981.	4.0	18
184	Surfaceâ€Mediated Interconnections of Nanoparticles in Cellulosic Fibrous Materials toward 3D Sensors. Advanced Materials, 2020, 32, e2002171.	21.0	18
185	Sustainable carboxylated cellulose filters for efficient removal and recovery of lanthanum. Environmental Research, 2020, 188, 109685.	7.5	18
186	Modification of carbon nanotubes with fluorinated ionic liquid for improving processability of fluoro-ethylene-propylene. European Polymer Journal, 2017, 87, 398-405.	5.4	17
187	Ionic Cross-Linked Poly(acrylonitrile- <i>co</i> -acrylic acid)/Polyacrylonitrile Thin Film Nanofibrous Composite Membrane with High Ultrafiltration Performance. Industrial & Engineering Chemistry Research, 2017, 56, 3077-3090.	3.7	17
188	High-flux anti-fouling nanofibrous composite ultrafiltration membranes containing negatively charged water channels. Journal of Membrane Science, 2020, 612, 118382.	8.2	17
189	Time-resolved simultaneous SAXS/WAXS studies of peek during isothermal crystallization, melting, and subsequent cooling. Journal of Macromolecular Science - Physics, 1998, 37, 667-682.	1.0	16
190	Phase Transitions and Honeycomb Morphology in an Incompatible Blend of Enantiomeric Polylactide Block Copolymers. Macromolecules, 2006, 39, 8203-8206.	4.8	16
191	Inducing Order from Disordered Copolymers: On Demand Generation of Triblock Morphologies Including Networks. Macromolecules, 2012, 45, 4599-4605.	4.8	16
192	A novel way to monitor the sequential destruction of parent-daughter crystals in isotactic polypropylene under uniaxial tension. Journal of Materials Science, 2014, 49, 3016-3024.	3.7	15
193	Decoration of Nanofibrous Paper Chemiresistors with Dendronized Nanoparticles toward Structurally Tunable Negativeâ€Going Response Characteristics to Human Breathing and Sweating. Advanced Materials Interfaces, 2017, 4, 1700380.	3.7	15
194	Enhancing Dehydration Performance of Isopropanol by Introducing Intermediate Layer into Sodium Alginate Nanofibrous Composite Pervaporation Membrane. Advanced Fiber Materials, 2019, 1, 137-151.	16.1	15
195	DEPENDENCE OF THE ONSET OF STRAIN-INDUCED CRYSTALLIZATION OF NATURAL RUBBER AND ITS SYNTHETIC ANALOGUE ON CROSSLINK AND ENTANGLEMENT BY USING SYNCHROTRON X-RAY. Rubber Chemistry and Technology, 2017, 90, 728-742.	1.2	14
196	An unusual promotion of Î ³ -crystals in metallocene-made isotactic polypropylene from orientational relaxation and favorable temperature window induced by shear. Polymer, 2018, 134, 196-203.	3.8	14
197	Influences of tacticity and molecular weight on crystallization kinetic and crystal morphology under isothermal crystallization: Evidence of tapering in lamellar width. Polymer, 2019, 172, 41-51.	3.8	14
198	Crystal structure changes during isothermal crystallization, cooling and heating of linear polyethylene. Journal of Polymer Research, 1999, 6, 167-173.	2.4	13

#	Article	IF	CITATIONS
199	Sequence distribution and elastic properties of propylene-based elastomers. Polymer, 2017, 111, 115-122.	3.8	13
200	The influence of short chain branch on formation of shear induced crystals in bimodal polyethylene at high shear temperatures. European Polymer Journal, 2018, 105, 359-369.	5.4	13
201	Electrospun Nanofibrous Membranes for Desalination. , 2019, , 81-104.		13
202	Morphological Changes During Crystallization and Melting of Polyoxymethylene Studied by Synchrotron X-Ray Scattering and Modulated Differential Scanning Calorimetry. Journal of Macromolecular Science - Physics, 2000, 39, 519-543.	1.0	12
203	A Synchrotron WAXD Study on the Early Stages of Coagulation during PBO Fiber Spinning. Macromolecules, 2002, 35, 9851-9853.	4.8	12
204	Uniaxial Deformation of Nylon 6–Clay Nanocomposites by In-Situ Synchrotron X-Ray Measurements. Journal of Macromolecular Science - Physics, 2003, 42, 201-214.	1.0	12
205	Development of Multiple-Jet Electrospinning Technology. ACS Symposium Series, 2006, , 91-105.	0.5	12
206	Structure Evolution upon Uniaxial Drawing Skin―and Core‣ayers of Injectionâ€Molded Isotactic Polypropylene by <i>In Situ</i> Synchrotron Xâ€ray Scattering. Journal of Polymer Science, Part B: Polymer Physics, 2013, 51, 1618-1631.	2.1	12
207	Complexation of DNA with cationic surfactants as studied by small-angle X-ray scattering. Science China Chemistry, 2014, 57, 1738-1745.	8.2	12
208	A Criterion for Flowâ€Induced Oriented Crystals in Isotactic Polypropylene under Pressure. Macromolecular Rapid Communications, 2017, 38, 1700407.	3.9	12
209	The influence of short chain branch on formation of shishâ€kebab crystals in bimodal polyethylene under shear at high temperatures. Journal of Polymer Science, Part B: Polymer Physics, 2018, 56, 786-794.	2.1	12
210	Hair test results at the advanced polymers beamline (X27C) at the NSLS. Synchrotron Radiation News, 1999, 12, 36-36.	0.8	11
211	Crystallization behavior of isotactic propyleneâ€1â€hexene random copolymer revealed by timeâ€resolved SAXS/WAXD techniques. Journal of Polymer Science, Part B: Polymer Physics, 2010, 48, 26-32.	2.1	11
212	Nanocellulose Extracted from Defoliation of Ginkgo Leaves. MRS Advances, 2018, 3, 2077-2088.	0.9	11
213	Nitro-oxidized carboxylated cellulose nanofiber based nanopapers and their PEM fuel cell performance. Sustainable Energy and Fuels, 2022, 6, 3669-3680.	4.9	11
214	Structural and Morphological Inhomogeneity of Short-Chain Branched Polyethylenes in Multiple-Step Crystallization. Journal of Macromolecular Science - Physics, 2000, 39, 317-331.	1.0	10
215	Polymeric nanofibrous composite membranes for energy efficient ethanol dehydration. Journal of Renewable and Sustainable Energy, 2012, 4, .	2.0	10
216	Microstructure and mechanical properties of isotactic polypropylene composite with twoâ€scale reinforcement. Polymers for Advanced Technologies, 2012, 23, 1580-1589.	3.2	10

#	Article	IF	CITATIONS
217	Current Advances on Nanofiber Membranes for Water Purification Applications. , 2018, , 25-46.		10
218	Ultraporous poly(lactic acid) scaffolds with improved mechanical performance using highâ€pressure molding and salt leaching. Journal of Applied Polymer Science, 2013, 130, 3509-3520.	2.6	9
219	The influence of short chain branch on formation of shear-induced crystals in bimodal polyethylene at low shear temperatures. Polymer, 2019, 179, 121625.	3.8	9
220	Ordering kinetics of body-centered-cubic morphology in diblock copolymer solutions at low temperatures. Journal of Rheology, 2004, 48, 1389-1405.	2.6	8
221	Functionalized bioâ€adsorbents for removal of perfluoroalkyl substances: A perspective. AWWA Water Science, 2021, 3, .	2.1	8
222	Crystallization study of poly(ether ether ketone)/poly(ether imide) blends by real-time small-angle x-ray scattering. Journal of Macromolecular Science - Physics, 1998, 37, 365-374.	1.0	7
223	Determination of Poly(4,4′â€diphenylsulfonyl terephthalamide) Crystalline Structure Via WAXD and Molecular Simulations. Macromolecular Chemistry and Physics, 2013, 214, 2432-2438.	2.2	7
224	Sulfonylcalix[4]arene functionalized nanofiber membranes for effective removal and selective fluorescence recognition of terbium(<scp>iii</scp>) ions. New Journal of Chemistry, 2018, 42, 6191-6202.	2.8	7
225	Temperature rising elution fractionation and fraction compositional analysis of Polybutene-1/Polypropylene in-reactor alloys. Materials Today Communications, 2020, 23, 100868.	1.9	7
226	Remediation of UO ₂ ²⁺ from Water by Nitro-Oxidized Carboxycellulose Nanofibers: Performance and Mechanism. ACS Symposium Series, 2020, , 269-283.	0.5	7
227	Electrospun Nanofibrous Adsorption Membranes for Wastewater Treatment: Mechanical Strength Enhancement. Chemical Research in Chinese Universities, 2021, 37, 355-365.	2.6	7
228	Morphology and mechanical properties of heterophasic PP–EP/EVA/organoclay nanocomposites. Journal of Applied Polymer Science, 2013, 128, 3473-3479.	2.6	6
229	Nanoparticle Based Printed Sensors on Paper for Detecting Chemical Species. , 2017, , .		6
230	Synthesis and characterization of poly(ethylene oxide)/polylactide/polylysine triâ€arm star copolymers for gene delivery. Journal of Polymer Science Part A, 2018, 56, 635-644.	2.3	6
231	Shear induced crystallization of bimodal and unimodal high density polyethylene. Polymer, 2018, 153, 223-231.	3.8	6
232	In situ synchrotron X-ray scattering studies on the temperature dependence of oriented β-crystal growth in isotactic polypropylene. Polymer Testing, 2020, 90, 106660.	4.8	6
233	Shear-free mixing to achieve accurate temporospatial nanoscale kinetics through scanning-SAXS: ion-induced phase transition of dispersed cellulose nanocrystals. Lab on A Chip, 2021, 21, 1084-1095.	6.0	6
234	Nano-Filamented Textile Sensor Platform with High Structure Sensitivity. ACS Applied Materials & Interfaces, 2022, 14, 15391-15400.	8.0	6

#	Article	IF	CITATIONS
235	Real-Time Crystallization and Melting Study of Ethylene-Based Copolymers by SAXS, WAXD, and DSC Techniques. ACS Symposium Series, 1999, , 187-200.	0.5	5
236	Isothermal Thickening and Thinning Processes in Low Molecular Weight Poly(ethylene oxide) Fractions Crystallized from the Melt. ACS Symposium Series, 1999, , 118-139.	0.5	5
237	Shear Enhanced Crystallization and Tensile Behaviors of Oscillation Shear Injection Molded Poly(ethylene terephthalate). Journal of Macromolecular Science - Physics, 2010, 50, 383-397.	1.0	5
238	Development of internal fine structure in stretched rubber vulcanizates. Journal of Polymer Science, Part B: Polymer Physics, 2011, 49, 1157-1162.	2.1	5
239	High-pressure crystallization of poly(lactic acid) with and without N2 atmosphere protection. Journal of Materials Science, 2013, 48, 7374-7383.	3.7	5
240	The supramolecular structure of bone: X-ray scattering analysis and lateral structure modeling. Acta Crystallographica Section D: Structural Biology, 2016, 72, 986-996.	2.3	5
241	Comprehensive study on temperature-induced crystallisation and strain-induced crystallisation behaviours of natural rubber/isoprene rubber blends. Plastics, Rubber and Composites, 2017, 46, 290-300.	2.0	5
242	Sequential Oxidation on Wood and Its Application in Pb2+ Removal from Contaminated Water. Polysaccharides, 2021, 2, 245-256.	4.8	5
243	Understanding ion-induced assembly of cellulose nanofibrillar gels through shear-free mixing and in situ scanning-SAXS. Nanoscale Advances, 2021, 3, 4940-4951.	4.6	5
244	Study the Use of Activated Carbon and Bone Char on the Performance of Gravity Sand-Bag Water Filter. Membranes, 2021, 11, 868.	3.0	5
245	Anomalous rheology in a nanostructured diblock copolymer/hydrocarbon system and its kinetic origin. Journal of Polymer Science, Part B: Polymer Physics, 2004, 42, 1496-1505.	2.1	4
246	Deformation X-ray study of propylene-based elastomers with controlled sequence distributions. Polymer, 2017, 122, 208-221.	3.8	4
247	Colorful nanofibrous composite membranes by two-nozzle electrospinning. Materials Today Communications, 2019, 21, 100643.	1.9	4
248	Cellulose-Supported Nanosized Zinc Oxide: Highly Efficient Bionanomaterial for Removal of Arsenic from Water. ACS Symposium Series, 2020, , 253-267.	0.5	4
249	The Influence of Ethyl Branch on Formation of Shish-Kebab Crystals in Bimodal Polyethylene under Shear at Low Temperature. Chinese Journal of Polymer Science (English Edition), 2021, 39, 1050-1058.	3.8	4
250	Time-resolved structural studies in fiber processing. Macromolecular Symposia, 2003, 195, 297-302.	0.7	3
251	Epitaxial Phase Transformation between Cylindrical and Double Gyroid Mesophases. Materials Research Society Symposia Proceedings, 2004, 856, BB2.3.1.	0.1	1
252	Continuous Production of Hollow Hydrogel Fibers with Graphene Inner Wall. Materials Science Forum, 0, 898, 2197-2204.	0.3	1

#	Article	IF	CITATIONS
253	A thirst for advancement. Nature Materials, 2018, 17, 213-215.	27.5	1
254	Effect of Sorbitol Templates on the Preferential Crystallographic Growth of Isotactic Polypropylene Wax. Crystals, 2018, 8, 59.	2.2	1
255	Effect of miscible polymer diluents on the development of lamellar morphology in poly(oxymethylene) blends. Journal of Polymer Science, Part B: Polymer Physics, 1999, 37, 3115-3122.	2.1	1
256	Lamellar crystal-dominated surfaces of polymer films achieved <i>via</i> melt stretching-induced free surface crystallization. Soft Matter, 2021, 17, 10829-10838.	2.7	1
257	Meeting Report: Soft Matter and Biomolecular Materials: X-ray Scattering Enabled by High Brightness Beamlines. Synchrotron Radiation News, 2006, 19, 43-44.	0.8	0
258	Structure, Morphology, and Mechanical Properties of Polyolefin-Based Elastomers. , 0, , 198-223.		0
259	Cellulose Nanofibers: Elucidating the Opportunities and Challenges for Nanocellulose Spinning (Adv.) Tj ETQq1 1	0.784314 21.0	rgBT /Overic
260	Static and Dynamic Light Scattering. World Scientific Series in Nanoscience and Nanotechnology, 2019, , 335-374.	0.1	0
261	Plant-derived carboxycellulose: Highly efficient bionanomaterials for removal of toxic lead from contaminated water. Separation Science and Technology, 2022, , 87-95.	0.2	0
262	Nitro-oxidation process for fabrication of efficient bioadsorbent from lignocellulosic biomass by combined liquid-gas phase treatment. Carbohydrate Polymer Technologies and Applications, 2022, 3, 100219.	2.6	0